Multifunctional Role of Tyr 108 in the Catalytic Mechanism of Human Glutathione Transferase P1-1. Crystallographic and Kinetic Studies on the Y108F Mutant Enzyme[†,‡]

Mario Lo Bello,*[,§] Aaron J. Oakley,[||] Andrea Battistoni,[§] Anna P. Mazzetti,[§] Marzia Nuccetelli,[§] Giampiero Mazzarese,[§] Jamie Rossjohn,[||] Michael W. Parker,[||] and Giorgio Ricci*[,§]

Department of Biology, University of Rome "Tor Vergata", Via della Ricerca Scientifica, 00133 Rome, Italy, and The Ian Potter Foundation Protein Crystallography Laboratory, St. Vincent's Institute of Medical Research, 41 Victoria Parade, Fitzroy, Victoria 3065, Australia

Received November 13, 1996; Revised Manuscript Received January 28, 1997[⊗]

ABSTRACT: The possible role of the hydroxyl group of Tyr 108 in the catalytic mechanism of human glutathione transferase P1-1 has been investigated by means of site-directed mutagenesis, steady-state kinetic analysis, and crystallographic studies. Three representative cosubstrates have been used, i.e. ethacrynic acid, 7-chloro-4-nitrobenz-2-oxa-1,3-diazole, and 1-chloro-2,4-dinitrobenzene. In the presence of ethacrynic acid, the enzyme follows a rapid equilibrium random bi−bi mechanism with a rate-limiting step which occurs after the addition of the substrates and before the release of products. The replacement of Tyr 108 with Phe yields a 14-fold decrease of k_{cat}, while it does not change appreciably the affinity of the H site for the substrate. In this case, it would appear that the role of the hydroxyl function is to stabilize the transition state for the chemical step, i.e. the Michael addition of GSH to the electrophilic substrate. Crystallographic data are compatible with this conclusion showing the hydroxyl group of Y108 in hydrogen bonding distance of the ketone moiety of ethacrynic acid [Oakley, A. J., Rossjohn, J., Lo Bello, M., Caccuri, A. M., Federici, G., & Parker, M. W. (1997) *Biochemistry 36*, 576−585]. Moreover, no structural differences are observed between the Y108F mutant and the wild type, suggesting that the removal of the hydroxyl group is solely responsible for the loss of activity. A different involvement of Tyr 108 appears in the catalyzed conjugation of 7-chloro-4-nitrobenz-2-oxa-1,3-diazole with GSH in which the rate-limiting step is of a physical nature, probably a structural transition of the ternary complex. The substitution of Tyr 108 yields an approximately 7-fold increase of k_{cat} and a constant k_{cat}/K_m^{NBD-Cl} value. Lack of a critical hydrogen bond between 7-chloro-4-nitrobenz-2-oxa-1,3-diazole and Tyr 108 appears to be the basis of the increased k_{cat}. In the 1-chloro-2,4-dinitrobenzene/GSH system, no appreciable changes of kinetics parameters are found in the Y108F mutant. We conclude that Y108 has a multifunctional role in glutathione transferase P1-1 catalysis, depending on the nature of the electrophilic cosubstrate.

The glutathione transferases (EC 2.5.1.18) (GSTs)[1] are a family of enzymes involved in the mechanism of cellular detoxification. They catalyze the nucleophilic attack of glutathione on the electrophilic center of a number of toxic compounds and xenobiotics (Jakoby & Habig, 1980). The cytosolic enzymes have been grouped into four species-independent classes: (alpha, mu, pi, and theta) on the basis of N-terminal sequence, substrate specificity, and immunological properties (Mannervik *et al*., 1985; Meyer *et al*., 1991). Very recently, a new class (sigma) has been proposed on the basis of primary structure, three-dimensional structure, and catalytic properties of a glutathione transferase from squid (Buetler & Eaton, 1992; Ji *et al*., 1995).

Human placental glutathione transferase (class pi) (GST P1-1) (Mannervik *et al*., 1992), a homodimeric protein of about 46 kDa, has been extensively studied in different laboratories because of clinical interest in it as a potential marker during chemical carcinogenesis (Kano *et al*., 1987; Tsuchida *et al*., 1989) and its potential role in the mechanism of cellular multidrug resistance against a number of antineoplastic agents (Batist *et al*., 1986; Black *et al*., 1990; Puchalski & Fahl, 1990). A number of amino acid residues involved in the binding of GSH have been identified by crystallographic analysis (Reinemer *et al*., 1992) and site-directed mutagenesis studies (Manoharan *et al*., 1992; Widersten *et al*., 1992; Kong *et al*., 1992). All these studies indicate that this site is specific for glutathione and several residues are involved in the substrate recognition. It is apparent that the same or similar residues are involved in

[†] Financial support from the National Research Council (96.03710.CT14) and the Anti-Cancer Council of Victoria is gratefully acknowledged. A.J.O. is a recipient of a National Health & Medical Research Council Postgraduate Research Scholarship. J.R. is a recipient of a Royal Society Fellowship. M.W.P. is a Wellcome Australian Senior Research Fellow.

[‡] The crystallographic coordinates have been deposited in the Brookhaven Protein Data Bank under the file name 4GSS.

* Address correspondence to these authors.

[§] Universityof Rome "Tor Vergata".

[||] St. Vincent's Institute of Medical Research.

[⊗] Abstract published in *Advance ACS Abstracts,* March 1, 1997.

[1] Abbreviations: CDNB, 1-chloro-2,4-dinitrobenzene; DMSO, dimethyl sulfoxide; DTNB, 5,5′-dithiobis(2-nitrobenzoic acid); DTT, 1,4-dithiothreitol; EA, ethacrynic acid; GS-EA, glutathione conjugate of ethacrynic acid; EDTA, ethylenediaminetetraacetic acid; 4-FSB, 4-(fluorosulfonyl)benzoic acid; GSH, glutathione; GST, glutathione transferase; LB, Luria broth; MES, 2-(*N*-morpholino)ethanesulfonic acid; NBC, *p*-nitrobenzyl chloride; NBD-Cl, 7-chloro-4-nitrobenz-2-oxa-1,3-diazole; 4-NQO, 4-nitroquinoline 1-oxide; SDS−PAGE, sodium dodecyl sulfate−polyacrylamide gel electrophoresis; WT, wild-type.

S0006-2960(96)02813-9 CCC: $14.00 © 1997 American Chemical Society

the binding of GSH in the other classes (Armstrong, 1994). On the contrary, three-dimensional structures of all five GST classes [alpha (Sinning *et al*., 1993), mu (Ji *et al*., 1992), pi (Reinemer *et al*., 1991, 1992), theta (Wilce *et al*., 1995), and sigma (Ji *et al*., 1995)] show that the binding site for the electrophilic substrate (H site) is quite different among them and very little is known about the key determinants of xenobiotic substrate specificity. So far, only a few amino acid residues have been identified as key determinants of the H site: Tyr 115, involved in the catalysis of rat mu GST (isoenzymes 3-3 and 4-4) (Johnson *et al*., 1993; Ji *et al*., 1994); Met 208, involved in the catalysis of GST A1-1 (Widersten *et al*., 1994); Ile 104 in GST P1-1 (Zimniak *et al*., 1994); and Val 10, Arg 11, and Val 104 in the murine class pi GST (Bammler *et al*., 1995).

In order to map the hydrophobic binding site of GST P1-1, we have started site-directed mutagenesis studies using as primary targets the residues which contribute to the formation of the hydrophobic pocket, as suggested by crystallographic analysis of GST P1-1, complexed with *S*-hexylglutathione (Reinemer *et al*., 1992). Tyr 108, the equivalent to Tyr 115 in class mu, is positioned in close contact to the hydrophobic substrate (less than 4 Å) and is a possible candidate for involvement in catalysis. In the present study, this residue has been mutated to phenylalanine. The mutant enzyme has been expressed in *Escherichia coli*, purified by affinity chromatography, and characterized with respect to its enzymatic properties, toward three selected substrates, i.e. ethacrynic acid (EA), 7-chloro-4-nitrobenz-2-oxa-1,3-diazole (NBD-Cl), and 1-chloro-2,4-dinitrobenzene (CDNB). The results show that Tyr 108 plays very different roles depending upon the nature of the electrophilic cosubstrate. The crystal structure of the Y108F mutant in complex with *S*-hexyl-GSH, determined to 2.5 Å resolution, and molecular modeling help explain this differential behavior.

EXPERIMENTAL PROCEDURES

Expression Plasmids and Site-Directed Mutagenesis. The plasmid pGST-1, producing large amounts of recombinant wild-type GST P1-1 in the cytoplasm of *E. coli*, has previously been described (Battistoni *et al*., 1995). The expression plasmid pGST-4 was obtained by inserting a 2350 bp *Eco*RI−*Sph*I DNA fragment from the plasmid pGST-1 (containing the lacI^q gene, the *trc* promoter, and the complete GST P1-1 sequence) into the corresponding sites of plasmid pEMBL18(+). This vector, which directs the synthesis of GST P1-1 in the cytoplasm of *E. coli* to an extent that is comparable to that of pGST-1, was used to generate the single-stranded DNA template used for site-directed mutagenesis according to the method described by Kunkel and co-workers with minor modifications (Kunkel *et al*., 1990; Lo Bello *et al*., 1995). The oligonucleotide 5′-TAGTTG-GTGAAGATGAGGG was used as mutagenic primer for the Y108F mutation. The oligonucleotide and the single-stranded DNA were mixed in a 10/1 molar ratio in 20 mM Tris-HCl (pH 7.4), 2 mM $MgCl_2$, and 50 mM NaCl, heated at 90 °C for 2 min, and allowed to cool to room temperature at an approximate rate of cooling of 1 °C/min. The *in vitro* DNA polymerization was performed in 100 μL of 20 mM Tris-HCl (pH 7.5), 2 mM 1,4-dithiothreitol (DTT), dATP, dCTP, dGTP, and dTTP (50 μL each), 0.4 mM ATP, 1 unit of native T7 DNA polymerase, and 2 units of T4 DNA ligase. After 1 h at 37 °C, the reaction was stopped by the addition of 15 mM EDTA. The mixture was used to transform competent BMH 71/18 mutS *E. coli* cells (Kramer *et al*., 1984) that were inoculated in Luria broth (LB) medium and incubated overnight at 37 °C. Plasmid DNA was extracted and newly transformed in BMH 71/18 cells that were plated on LB/ampicillin in order to obtain segregation of mutant and wild-type plasmids. Colonies containing the mutated plasmid were identified by colony hybridization. The nucleotide sequence of the plasmid carrying the Y108F mutation (pGST-F108) was verified by the dideoxy chain termination method.

Scheme 1

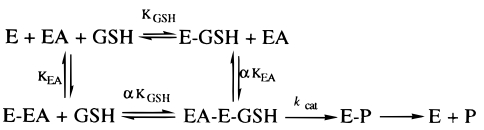

Protein Expression and Purification. Wild-type and mutant GST P1-1 were produced as previously described (Lo Bello *et al*., 1995; Battistoni *et al*., 1995). Briefly, TOP 10 *E. coli* cells, harboring plasmid pGST-1 or plasmid pGST-F108, were grown in LB medium containing 100 μg/mL ampicillin and 50 mg/mL streptomycin. The synthesis of GST was induced by the addition of 0.2 mM isopropyl 1-thio-β-galactopyranoside when the absorbance at 600 nm was 0.5. Eighteen hours after induction, cells were harvested by centrifugation and lysed as previously described (Battistoni *et al.*, 1995). Wild-type and Y108F mutant GSTs were purified by affinity chromatography on immobilized glutathione (Simons & Van der Jagt, 1977). After affinity purification, the wild-type and the Y108F mutant enzymes were homogeneous as judged by SDS−PAGE (Laemmli, 1970). The protein concentration was determined by the method of Lowry *et al*. (1951).

Kinetic Studies. The enzymatic activities were determined spectrophotometrically at 25 °C with different cosubstrates under the conditions reported below. Spectrophotometric measurements were performed in a double-beam Uvicon 940 spectrophotometer (Kontron Instruments) equipped with a thermostated cuvette compartment. Initial rates were measured at 0.1 s intervals for a total period of 12 s after a lag time of 5 s. Enzymatic rates were corrected for the spontaneous reaction.

Kinetic experiments with EA were performed in 1 mL (final volume) of 0.1 M potassium phosphate buffer (pH 6.5) containing 1 mM EDTA, GSH (from 0.04 to 1 mM), EA (from 0.05 to 0.5 mM), and about 50 μg of GST P1-1. Kinetic data were collected by varying EA at a fixed GSH concentration (and vice versa) over a matrix of 48 substrate concentrations by following the increase of absorbance at 270 nm where the conjugate of EA with GSH (GS-EA) absorbs ($\epsilon_{270} = 5700\ M^{-1}\ cm^{-1}$) (Habig *et al*., 1974). The calculation of enzymatic activity was done by taking into account the decrease of absorbance at 270 nm due to the disappearance of EA ($\epsilon_{270} = 3200\ M^{-1}\ cm^{-1}$). Kinetic data were fitted to the simplest equation which describes the rapid equilibrium random sequential bi−bi model (eq 1, see Scheme 1):

$$v = V_{max}[GSH][EA]/(\alpha K_{GSH}K_{EA} + \alpha K_{GSH}[EA] + \alpha K_{EA}[GSH] + [GSH][EA]) \quad (1)$$

where v is the initial velocity, α is the coupling factor, K_{GSH}

is the dissociation constant of GSH, and K_{EA} is the dissociation constant for EA. The parameters to be varied in the fitting procedure were V_{max}, the coupling factor α, and K_{EA}, while a fixed K_{GSH} value has been used, on the basis of Ivanetich and Goold (1989).

Inhibition experiments with GS-EA were performed over a 35-substrate concentration matrix in the presence of fixed inhibitor concentrations ranging from 0 to 0.1 mM. Several sets of $1/v$ *versus* 1/[GSH] (or 1/[EA]) plots at various fixed GS-EA concentrations and constant EA concentrations (or GSH concentrations) were obtained. The slopes within each set are replotted against the corresponding GS-EA concentration. $K_{i(slope)}^{P/EA}$ and $K_{i(slope)}^{P/GSH}$, which represent the intercepts on the *x*-axis, are plotted *versus* the concentration of the fixed substrate.

Apparent kinetic parameters, k_{cat}, K_m^{cosub}, and k_{cat}/K_m^{cosub} (reported in Table 4), for different cosubstrates were determined at a fixed GSH concentration and with various cosubstrate concentrations, by fitting the collected data to the Michaelis−Menten equation by nonlinear regression analysis using the Graph PAD Prism (Graph PAD Software, San Diego, CA) computer programs. Experimental conditions for each substrate were (1) 0.05−0.5 mM EA in the presence of 1 mM GSH in 0.1 M potassium phosphate buffer at pH 6.5. The apparent K_m^{GSH} was obtained at a fixed EA concentration (0.5 mM) and various GSH concentrations (from 0.05 to 1 mM). (2) This set of conditions was 0.0025−0.5 mM NBD-Cl in the presence of 0.5 mM GSH in 0.1 M sodium acetate at pH 5.0; the reaction was monitored at 419 nm ($\epsilon = 14\,500\ M^{-1}\ cm^{-1}$) (Ricci *et al*., 1994). The apparent K_m^{GSH} was calculated in the same conditions at a fixed NBD-Cl concentration (0.2 mM) and various GSH concentrations (from 0.002 to 0.5 mM). (3) This set of conditions was 0.1−2 mM CDNB in the presence of 5 mM GSH in 0.1 M potassium phosphate buffer (pH 6.5) containing 0.1 mM EDTA; the reaction was monitored at 340 nm ($\epsilon = 9600\ M^{-1}\ cm^{-1}$) (Habig *et al*., 1974). The apparent K_m^{GSH} was also determined at a fixed CDNB concentration (1 mM) and various GSH concentrations (from 0.02 to 5 mM). (4) This set of conditions was 0.01−0.4 mM 5,5′-dithiobis(2-nitrobenzoic acid) (DTNB) in the presence of 0.4 mM GSH in 0.1 M sodium acetate buffer at pH 5.0; the reaction was monitored at 412 nm ($\epsilon = 13\,600\ M^{-1}\ cm^{-1}$) (Ellman, 1959). (5) This set of conditions was 0.025−0.3 mM 4-nitroquinoline 1-oxide (4-NQO) in the presence of 1 mM GSH in 0.1 M phosphate buffer at pH 6.5; the reaction was monitored at 350 nm ($\epsilon = 7200\ M^{-1}\ cm^{-1}$) (Stanley & Benson, 1988). (6) This set of conditions was 0.05−0.8 mM *p*-nitrobenzyl chloride (NBC) in the presence of 5 mM GSH in 0.1 M potassium phosphate buffer at pH 6.5; the reaction was monitored at 310 nm ($\epsilon = 1900\ M^{-1}\ cm^{-1}$) (Habig *et al*., 1974). Kinetic parameters reported in this paper represent the mean of at least three different experimental data sets.

The pH dependence of k_{cat} and k_{cat}/K_m for different cosubstrates was obtained by using 0.1 M sodium acetate buffers (from pH 4.0 to 5.5) and potassium phosphate buffers (from pH 6.0 to 7.5).

Viscosity Variation Experiments. The effect of viscosity on kinetic parameters was assayed by using 0.1 M potassium phosphate and 0.1 M sodium acetate buffers, both containing various glycerol concentrations. Viscosity values (η) at 25 °C were calculated from Wolf *et al*. (1985) and randomly controlled with an Ostwald viscosimeter. Viscosities are reported relative to 0.1 M potassium phosphate buffer at pH 6.5 and 0.1 M sodium acetate at pH 5.0.

Thermal Stability. The wild-type and Y108F mutant enzymes were incubated at different temperatures (range of 25−60 °C) for at least 30 min, at a protein concentration of 0.1 mg/ml in 0.1 M phosphate buffer (pH 6.5) containing 0.1 mM EDTA. At regular time intervals, aliquots were withdrawn from the incubation mixture and assayed for GST activity. The results (data not shown) showed that the thermal stability of the Y108F mutant enzyme was unaffected by replacement of Tyr with Phe.

Crystallization and Data Collection. Crystallization was performed by the hanging drop vapor diffusion method (McPherson, 1982) using 24-well tissue culture plates. A 2 μL droplet of protein solution (concentration between 7 and 12 mg/mL) containing 10 mM phosphate buffer (pH 7.0), 1 mM EDTA, and 2 mM mercaptoethanol was mixed with an equal volume of reservoir solution (as described below). Each well contained 1 mL of reservoir solution. Suitable crystals for X-ray diffraction experiments required the presence of the inhibitor *S*-hexylglutathione in the reservoir solution. The trials were carried out at a constant temperature of 22 °C.

Initial crystallization trials were performed using conditions similar to those for the wild-type crystallization (Parker *et al*., 1990). Crystals appeared in the shape of tetragonal prisms within 2−4 days using ammonium sulfate as a precipitant. The crystallization conditions varied from the published wild-type conditions (Parker *et al*., 1990) in two respects. Firstly, it was found that the presence of 100 mM DTT improved the crystal quality and has sometimes proved to be an essential ingredient in the crystallization of wild-type protein. Secondly, suitable crystals could only be obtained in the presence of certain organic compounds such as ethanol, dimethyl sulfoxide (DMSO), acetone, ethylene glycol, or 2-methylpentane-2,4-diol. The best additives were either 5−10% v/v ethanol or 5% DMSO. The crystals grown under these conditions tended to give highly mosaic diffraction patterns and diffracted barely past 3.0 Å resolution. We recently crystallized the wild-type protein in a new crystal form (A. J. Oakley *et al*., unpublished results) and subsequently found that the Y108F mutant yielded much better crystals which diffracted to greater than 2.5 Å resolution, under the new conditions. The optimal reservoir buffer consists of 29% (w/v) ammonium sulfate, 55 mM DTT, 7 mM *S*-hexylglutathione, 5% DMSO, and 100 mM 2-(*N*-morpholino)ethanesulfonic acid (MES) buffer at pH 5.8−6.0. The crystals grow as plates within 1 week with maximal dimensions of 0.3 mm × 0.5 mm × 0.5 mm.

The X-ray diffraction data were collected using a MAR-RESEARCH area detector with CuK_a X-rays generated by a Rigaku RU-200 rotating anode X-ray generator. The crystals were transferred in one step into reservoir solution containing 20% glycerol. The crystals were flash-frozen with an Oxford Cryosystems Cryostream cooler and the data collected at 100 K. The diffraction data were processed and analysed using programs in the HKL (Otwinowski, 1993) and CCP4 (1994) program suites. The relevant data statistics are presented in Table 1.

Structure Solution and Refinement. The initial analysis of the mutant included examination of difference Fourier maps calculated with SIGMAA-weighted $F_{mutant} - F_{native}$ and $2F_{mutant} - F_{native}$ coefficients (Read, 1986). Native amplitudes

Table 1: Crystallographic Data for the Glutathione Transferase Mutant Y108F

data	
space group	*C*2
cell dimensions	
a, *b*, and *c* (Å) and β (deg)	78.5, 90.3, 69.0, and 97.5
maximum resolution (Å)	2.5
no. of crystals	2
total no. of observations	79 944
no. of unique reflections	14 346
completeness of data (%)[a]	88.5 (90.0)
no. of data $>3\sigma_I$ (%)[a]	58.4 (38.2)
R_{merge} (%)[a]	11.1 (29.1)
refinement	
non-hydrogen atoms	3260 protein 52 *S*-hexyl-GSH inhibitor 189 water 24 MES buffer
$R_{conventional}$ (%)	20.4
R_{free} (%)	26.4
reflections used in *R* factor calculations (15.0−2.5 Å)	
number, completeness (%)	13 938, 84.5
rmsds from ideal geometry	
bonds (Å)	0.007
angles (deg)	1.30
dihedrals (deg)	22.1
impropers (deg)	1.2
residues in the most favorable regions of the Ramachandran plot (%)	93.6

[a] The values in parentheses are for the highest-resolution bin (2.60−2.50 Å).

and phases were derived from a model of the wild-type enzyme in the *C*2 space group (A. J. Oakley *et al.*, unpublished results). The $2F_{mutant} - F_{native}$ electron density maps were further improved by 2-fold noncrystallographic averaging using the MAMA (Kleywegt & Jones, 1994), RAVE (Kleywegt & Jones, 1994), and CCP4 (1994) program suites. Refinements began with the wild-type model, and rigid body refinement in XPLOR version 3.1 (Brünger *et al*., 1987) was used to compensate for any possible changes in crystal packing. The model was then subjected to simulated annealing and individual *B* factor refinement with XPLOR. Tight noncrystallographic symmetry restraints were used throughout the refinement.

Modeling Studies. Modeling was performed on a Silicon Graphics Indigo2 EXTREME workstation using the software-modeling package INSIGHT II (Biosym Technologies Inc., San Diego, CA). Molecular dynamics simulations and energy minimization calculations were performed using DISCOVER (Biosym Technologies Inc.). A model of NBD-Cl was built and energy minimized to tidy its geometry. The ligand was roughly positioned in the H site of the human GST P1-1 (Reinemer *et al*., 1992) so it was bound in a productive mode (i.e. the chlorine atom was positioned close to where the thiol group of the glutathione substrate would be located when bound). The rings of the ligand were orientated such that they were stacked in parallel fashion between the aromatic rings of Tyr 108 and Phe 8 as observed in other GST−ligand complexes (Garcìa-Sàez *et al.*, 1994; A. J. Oakley *et al*., unpublished results). This reduced the number of possible binding geometries to be explored to three general possibilities: two in which the nitro moiety pointed out toward solution (and the five-membered ring points either toward the H site or out toward the solvent) and the other where it pointed into the H site. The latter possibility was excluded because no favorable interactions with the nitro group could be found. Molecular dynamics simulation was performed on the remaining possibilities, followed by 200 steps of conjugate gradient energy minimization to relieve any residual strain and to optimize any potential electrostatic and van der Waals contacts. Of the two remaining possibilities, the five-membered ring pointing into the H site yielded more favorable protein−ligand interactions.

RESULTS

Crystallographic Analysis of the Y108F Crystals. The protein crystallized in space group *C*2 with the following cell dimensions: $a = 78.5$ Å, $b = 90.3$ Å, $c = 69.0$ Å, and $\beta = 97.5°$. There is a dimer in the asymmetric unit, and crystals diffracted to beyond 2.5 Å resolution. An 88.5% complete data set was collected from two frozen crystals with an overall R_{merge} of 11.1% (Table 1). The initial $2F_{mutant} - F_{native}$ electron density map was of sufficient quality to demonstrate the lack of any significant conformational change to the enzyme because of replacement of the tyrosine. Among the significant features found in the $F_{mutant} - F_{native}$ were negative peaks (approximately up to 6 times the rms error of the map) over the position of the hydroxyl group of Tyr 108 in both monomers, thus confirming the mutation and large positive peaks corresponding to *S*-hexylglutathione inhibitor which was not included in the phase calculation. The residue at position 108 was changed from tyrosine to phenylalanine and the model refined. After rigid body refinement, the conventional *R* factor was 41.9% ($R_{free} = 40.2\%$) for all data between 8.0 and 2.5 Å. After group *B* factor refinement and rebuilding, the inhibitor *S*-hexylglutathione was included in the model. The *R* factor was 28.8% ($R_{free} = 33.7\%$) at this stage. Following further rounds of refinement, individual restrained *B* factor refinement was carried out (conventional *R* factor = 27.2%, $R_{free} = 32.7\%$). A bulk solvent correction was applied and the model refined against all data between 15 and 2.5 Å resolution. In the final model, the conventional *R* factor is 20.4% and the free *R* value is 26.4% for all data between 15.0 and 2.5 Å (Table 1). The quality of the final map is excellent (Figure 1). A stereochemical analysis of the refined structure with the program PROCHECK (Laskowski *et al*., 1993) gave values either similar to or better than those expected for structures refined at 2.5 Å resolution.

The final model demonstrates that there are no significant differences between wild-type and mutant crystal structures (Figure 2) so any changes in the catalytic properties of Y108F are due solely to the removal of the hydroxyl group of Tyr 108.

Enzymatic Conjugation of GSH with Ethacrynic Acid. Ethacrynic acid (EA) is used in chemotherapeutic treatments to minimize drug resistance due to GST activity (Yang *et al*., 1992). EA is generally considered to be a GST inhibitor because most GST isoenzymes display low activity toward it. Some detailed studies have been performed to define its inhibitory action toward the classical CDNB/GSH reaction (Ploemen *et al*., 1990; Phillips & Mantle, 1991; Awasthi *et al*., 1993). Although the GST P1-1 enzyme has been shown to display activity toward EA, incomplete kinetic investigations have been performed using it as the substrate. It is evident that a steady-state kinetic characterization needs to be established for any other investigation concerning the enzymatic mechanism. As shown in Figure 3, sets of

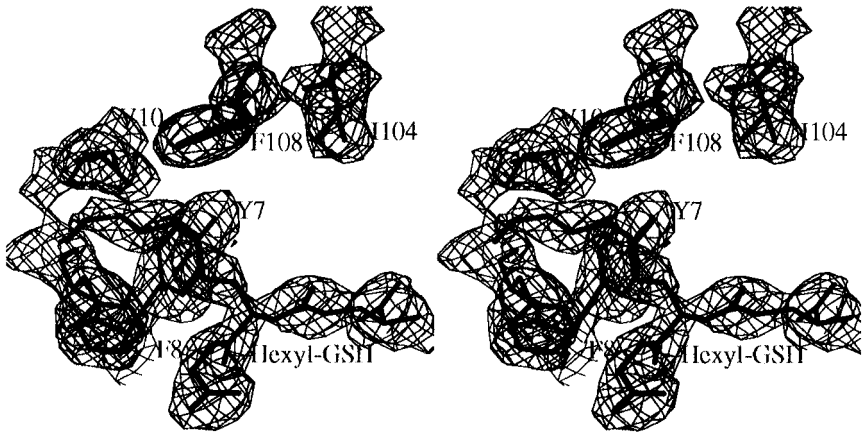

FIGURE 1: Stereodiagram of the final $2F_{mutant} - F_c$ electron density map of the Y108F mutant in the vicinity of the mutation. This map was calculated using all reflections between 40.0 and 2.5 Å and contoured at the 1σ level.

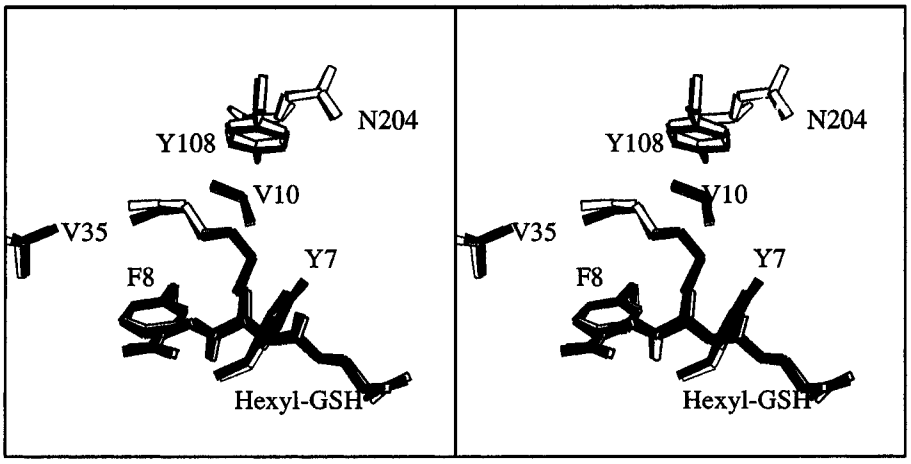

FIGURE 2: Superposition of the wild-type and Y108F mutant structures in the vicinity of mutation. Filled bonds are for the wild-type structure, and hollow bonds are for the mutant. The figure was generated with the program MOLSCRIPT (Kraulis, 1991).

reciprocal plots of initial velocities in the presence of a fixed GSH concentration and various EA concentrations (and *vice versa*) intercept just below the *x*-axis; these kinetic data were well fitted to the simplest rapid equilibrium random sequential bi−bi equation (see eq 1) or with the mathematically equivalent steady-state ordered bi−bi model (Segel, 1975) (mean square error = 5). Other reasonable models (rapid equilibrium ordered bi−bi mechanisms and steady-state random sequential mechanism) are less reliable on the basis of high mean square errors (>15). Product inhibition studies with GS-EA allows discrimination between the two possible mechanisms. GS-EA is a competitive inhibitor toward both GSH and EA (data not shown), and the replots of inhibition data, performed as described in Experimental Procedures, are diagnostic for the rapid equilibrium model (Segel, 1975) (Figure 4, see Scheme 1).

Kinetic parameters obtained by the fitting procedures are reported in Table 2. Kinetic data are also consistent with a negative synergistic modulation of one substrate on the binding of the second one (coupling factor $\alpha = 1.6$). Viscosity variation experiments shed light on the rate-limiting step of this reaction. As reported in Table 3, an increased viscosity by glycerol does not yield any change of the k_{cat} value so we can exclude the release of GS-EA or diffusionally controlled structural transitions as rate-determining steps.

Effect of Replacement of Tyr 108 with Phe on the Conjugation of EA. The substitution of Tyr 108 with Phe yields a marked decrease of the k_{cat} value which is 14-fold lower than that found with WT (Table 4). On the contrary, no remarkable changes in both K_m^{GSH} and K_m^{EA} have been found. Due to the rapid equilibrium mechanism, the invariance of K_m values in WT and mutant must be related to an unchanged thermodynamic binding affinity constant (K_d) for both EA and GSH. The catalytic efficiency k_{cat}/K_m^{EA}, which is 12.2 mM^{-1} s^{-1} in the WT enzyme, is 0.94 mM^{-1} s^{-1} in the mutant. Similarly, k_{cat}/K_m^{GSH} is also lowered from 14.5 mM^{-1} s^{-1} (WT) to 1 mM^{-1} s^{-1} in Y108F. These lowered k_{cat}/K_m values in Y108F rule out the possibility that replacement of Tyr 108 caused a nonproductive binding of EA or GSH at the active site in the ternary complex. The pH dependence of k_{cat} for Y108F, explored between pH 5 and 8, is also very similar to that found for WT and identifies a kinetically relevant ionization in the ternary complex with a pK_a of 6.22 ± 0.08 (6.36 ± 0.06 for WT) (data not shown). As previously suggested (Ji *et al*., 1995), this pK_a is likely

Table 2: Kinetic Parameters and Dissociation Constants for EA/GSH Conjugation by GST P1-1[a]

K_{EA} (mM)	0.140 ± 0.008
K_{GSH} (mM)	0.125 ± 0.006
α	1.6 ± 0.1
V_{max}	1.20 ± 0.01

[a] K_{GSH} is the dissociation constant as reported by Ivanetich and Goold (1989). K_{EA}, the coupling factor α, and V_{max} (expressed as ΔA_{270nm}/min with 0.05 mg of GST P1-1) are derived by fitting the kinetic data (shown in Figure 3) to eq 1.

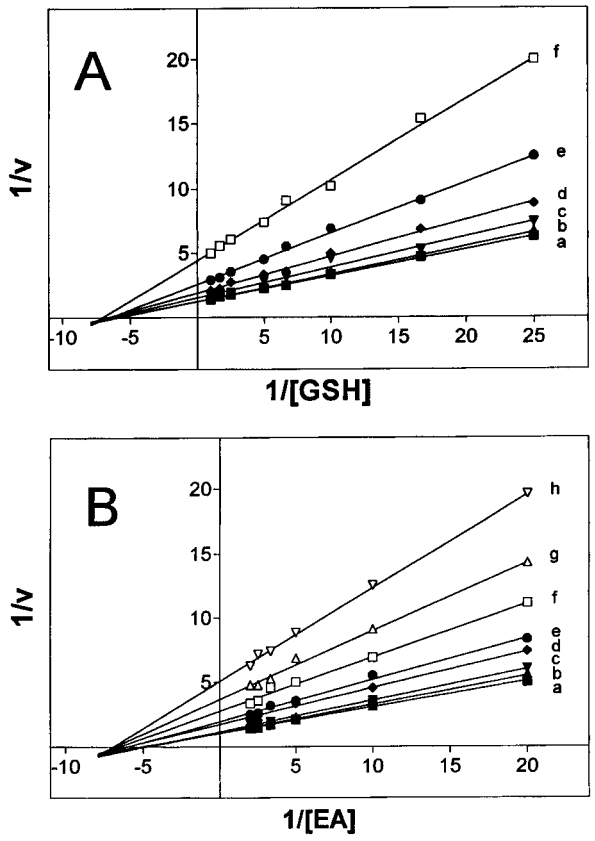

FIGURE 3: Double-reciprocal plots for the EA/GSH conjugation by GST P1-1. Assay conditions and data analysis are reported in Experimental Procedures. (A) With GSH as the varied substrate, EA concentrations (millimolar) were 0.5 (a), 0.4 (b), 0.3 (c), 0.2 (d), 0.1 (e), and 0.05 (f). (B) With EA as the varied substrate, GSH concentrations (millimolar) were 1 (a), 0.6 (b), 0.4 (c), 0.2 (d), 0.15 (e), 0.1 (f), 0.06 (g), and 0.04 (h). Velocities are expressed as ΔA_{270nm}/min.

due to the sulfhydryl group deprotonation of the bound GSH which therefore seems unaffected by this point mutation. Like the WT enzyme, the Y108 mutant displays no change of the k_{cat} value when the viscosity is increased with glycerol (Table 3).

Table 3: Viscosity Effect on Kinetic Parameters of Y108F and WT toward Selected Substrates[a]

substrate	enzyme	$k_{cat}°/k_{cat}$ ($\eta/\eta° = 3.83$)	α
EA	WT	1	0.02 ± 0.01
	Y108F	1	0.01 ± 0.01
CDNB	WT	3.3	0.81 ± 0.04
	Y108F	3.4	0.86 ± 0.06
NBD-Cl	WT	1.2	0.07 ± 0.02
	Y108F	2.1	0.38 ± 0.03

[a] $k_{cat}°$ represents the turnover number when the relative viscosity ($\eta/\eta°$) is 1; k_{cat} is the experimental value observed when the relative viscosity is 3.83, with glycerol as the cosolvent. α is the slope of the dependence of $k_{cat}°/k_{cat}$ on $\eta/\eta°$ (varied from 1 to 3.83) as derived from the best linear fit of the experimental data.

Effect of Replacement of Tyr 108 on the Conjugation of NBD-Cl. NBD-Cl is a poor cosubstrate for GST P1-1, and its conjugation rate with GSH is about 70-fold lower than that in the GSH/CDNB system (Table 4). Even with this substrate, GST follows a rapid equilibrium random bi−bi mechanism, but the rate-limiting step seems to be related to a conformational transition of the ternary complex which probably involves helix 4 (Caccuri *et al*., 1996). A strong synergistic modulation between G and H sites also occurs so the affinity for GSH increases about 30 times at saturating cosubstrate (α = 0.036) (Caccuri *et al*., 1996). Removal of the hydroxyl group of Tyr 108 yields an increased catalytic efficiency and a lowered affinity toward GSH and NBD-Cl. In particular, the k_{cat} value increases about 7-fold while K_m^{GSH} (8 μM in the WT) becomes 55 μM in the mutant (Table 4). Similarly, K_m^{NBD-Cl} increases from 4 to 32 μM. The possible influence of the hydroxyl group of Tyr 108 on the pK_a values of kinetically relevant ionizations was also checked by studying the pH dependence of k_{cat} and k_{cat}/K_m^{NBD-Cl}. The turnover number of WT is pH-independent (between pH 4.2 and 6.5), while in Y108F, it decreases below

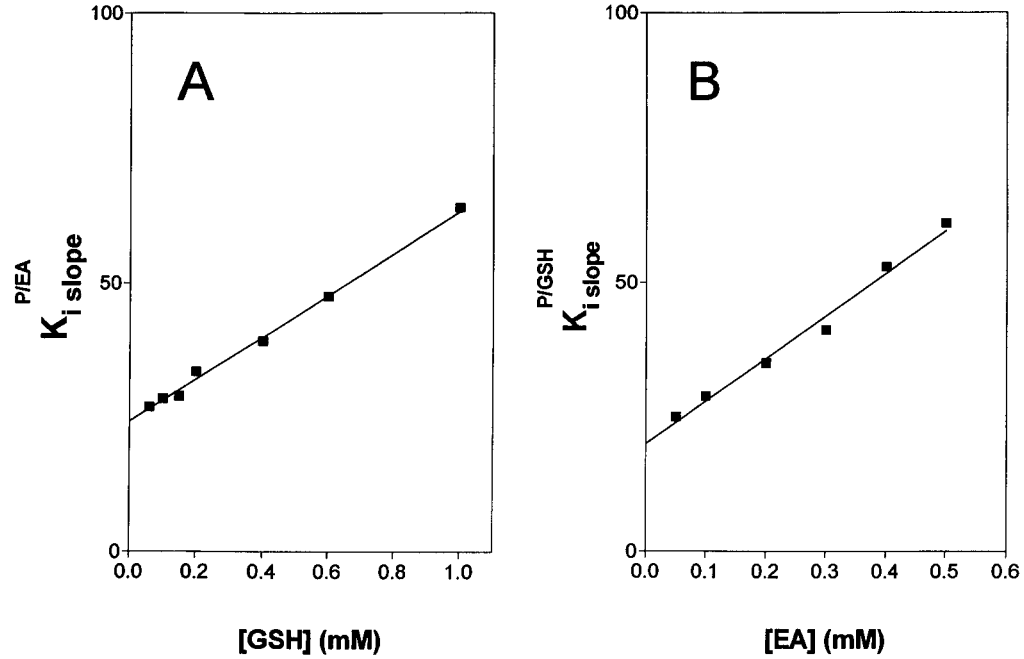

FIGURE 4: Secondary plots of GS-EA inhibition on EA/GSH conjugation by GST P1-1. Secondary plots of $K_{i(slope)}^{P/EA}$ *versus* [GSH] (A) and $K_{i(slope)}^{P/GSH}$ *versus* [EA] (B) are obtained from a set of reciprocal plots at different fixed concentrations of GS-EA (with EA as the varied substrate and fixed GSH concentrations and vice versa) as reported in Experimental Procedures.

Table 4: Steady-State Kinetic Parameters of GST P1-1 WT and Y108F with Selected Hydrophobic Substrates[a]

substrate	enzyme	k_{cat} (s^{-1})	K_m^{GSH} (mM)	K_m^{cosub} (mM)	k_{cat}/K_m^{cosub} (s^{-1} mM^{-1})
EA	WT	2.57 ± 0.01	0.177 ± 0.006	0.21 ± 0.02	12.2 ± 0.8
	Y108F	0.18 ± 0.02	0.18 ± 0.01	0.19 ± 0.02	0.94 ± 0.9
NBD-Cl	WT	1.1 ± 0.2	0.008 ± 0.002	0.004 ± 0.001	275 ± 12
	Y108F	7.9 ± 0.2	0.055 ± 0.004	0.032 ± 0.005	247 ± 16
CDNB	WT	76 ± 2	0.15 ± 0.03	1.2 ± 0.1	63 ± 2
	Y108F	65 ± 1	0.15 ± 0.04	0.97 ± 0.07	67 ± 4
4-NQO	WT	73 ± 2	nd[b]	0.33 ± 0.03	222 ± 20
	Y108F	21 ± 3	nd	0.31 ± 0.03	67 ± 6
DTNB	WT	6.2 ± 0.1	nd	0.053 ± 0.09	117 ± 8
	Y108F	5.6 ± 0.2	nd	0.048 ± 0.004	116 ± 5
NBC	WT	0.23 ± 0.05	nd	0.51 ± 0.12	0.45 ± 0.04
	Y108F	1.0 ± 0.1	nd	0.48 ± 0.1	2.1 ± 0.2

[a] Apparent kinetic parameters were calculated as described in Experimental Procedures. [b] Not detected.

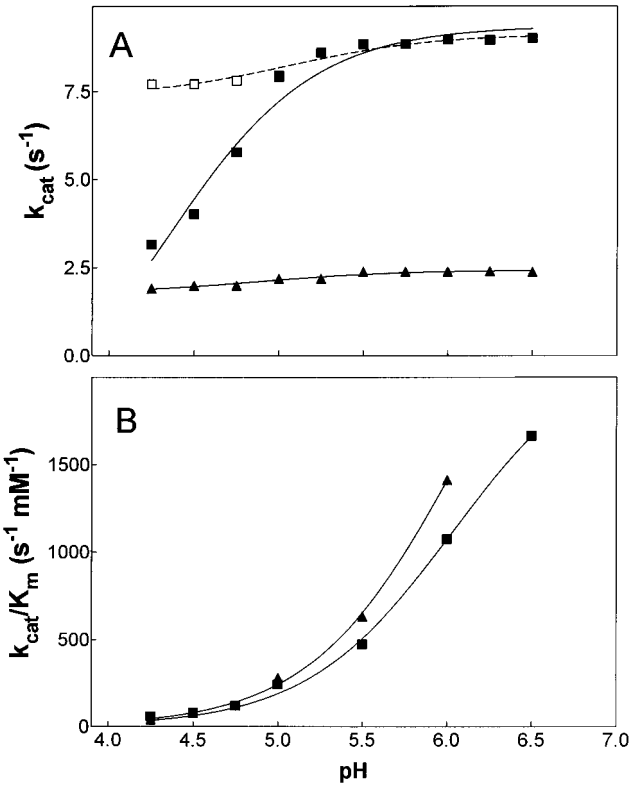

FIGURE 5: pH dependence of kinetic parameters for NBD-Cl/GSH conjugation. The solid lines are computer fits of the experimental data with Y108F (■) and WT (▲) GST P1-1 to the equations $k_{cat} = k_{cat}^{lim}/(1 + 10^{-pH}/K_a)$ (A) and $k_{cat}/K_m^{NBD-Cl} = (k_{cat}/K_m^{NBD-Cl})^{lim}/(1 + 10^{-pH}/K_a)$ (B). The k_{cat} values in panel A for the wild-type enzyme were multiplied 2-fold to facilitate comparison with those of Y108F. The solid line for k_{cat} of WT in panel A only represents the average value. Experiments were performed as described in Experimental Procedures. k_{cat}^{lim} and the apparent pK_a values for Y108F (A) were 9.1 s^{-1} and 4.5, respectively. k_{cat} values for Y108F, measured at pH 5.0 after a short preincubation at pH 4.25, 4.50, and 4.75, respectively, are very similar to that obtained at these specific pH values. k_{cat} values, corrected for this irreversible pH-dependent inactivation, are shown as hollow squares. The pK_a values in panel B, calculated by computer fits, were ≥6.2 for both WT and Y108F.

pH 5.0 (Figure 5A). However, the lowered k_{cat} values observed below pH 5.0 are due to an irreversible pH-dependent inactivation (as checked by a short preincubation of the enzyme at the given pH and subsequent activity determination at pH 5.0) and cannot be ascribed to reversible ionizations occurring in the ternary complex. Kinetic data, corrected for this aspecific inactivation, show that no relevant reversible ionizations occur in the rate-limiting step of Y108F

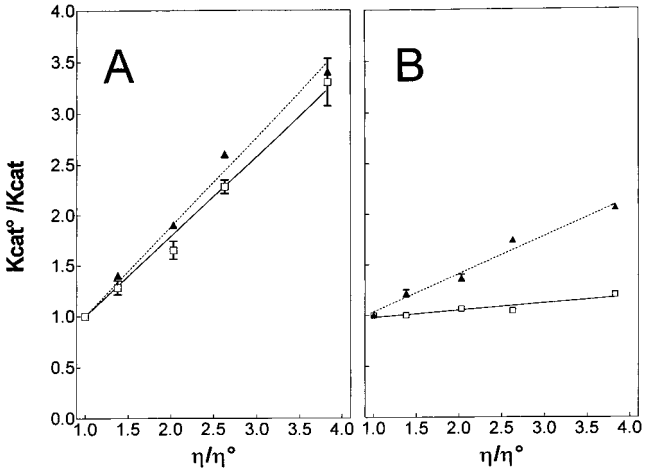

FIGURE 6: Viscosity effect on kinetic parameters of wild-type and Y108F mutant enzymes. Dependence of the reciprocal of the relative turnover numbers ($k_{cat}°/k_{cat}$) on the relative viscosity ($\eta/\eta°$) for CDNB as the cosubstrate (A) with the native enzyme (□) and the Y108F mutant (▲) and for NBD-Cl as the cosubstrate (B) with the native enzyme (□) and Y108F mutant (▲). Kinetic data for the enzymatic reactions were obtained as described in Experimental Procedures. Slopes of linear fits are 0.81 and 0.86 with the native and Y108F mutant enzymes, respectively, with CDNB as the substrate, and 0.07 and 0.38 with the native and Y108F mutant enzymes, respectively, with NBD-Cl as the substrate.

(see Figure 5A). Moreover, a similar pH dependence of k_{cat}/K_m^{NBD-Cl}, at saturating GSH concentrations, has been seen for WT and Y108F (Figure 5B). Although experimental conditions above pH 6.5 cannot be used for the high rate of the spontaneous reaction, a pK_a value of ≥6.2 can be calculated. This pK_a may be related to the ionization of GSH in the binary complex (Liu *et al*., 1992).

Interesting results come from viscosity experiments. While there is no substantial effect of the viscosity on k_{cat} for the wild-type enzyme (slope of $k_{cat}°/k_{cat} = 0.07$), the k_{cat} value for the Y108F mutant enzyme is significantly lowered by an increased viscosity, giving a slope of $k_{cat}°/k_{cat}$ of 0.38 (Table 3 and Figure 6).

Effect of Replacement of Tyr 108 on the Conjugation of CDNB and Other Substrates. The effect of the point mutation in Tyr 108 on the conjugation reaction of GSH with CDNB is negligible. Both k_{cat} and K_m^{GSH} and K_m^{CDNB} values remain essentially unchanged (Table 4) as well as the dependence of k_{cat} on pH (data not shown). A similar invariance of kinetic parameters was obtained with DTNB as the cosubstrate which displays k_{cat} values of 6.2 and 5.6

s^{-1} in the WT and Y108F mutant, respectively (Table 4). On the contrary, other substrates behave like EA. For example, 4-NQO, which is a good cosubstrate for GST P1-1 ($k_{cat} = 73\ s^{-1}$, $K_m = 0.33$ mM), is conjugated about 3.5-fold more slowly in the Y108 mutant without any change of the K_m value (Table 4). With NBC as the cosubstrate, the removal of the hydroxyl group causes a 4-fold increase of k_{cat} (from 0.23 to 1 s^{-1}), and this behavior resembles that of NBD-Cl (Table 4).

DISCUSSION

Tyr 108 is located near the top of helix 4, and its aromatic ring is nestled in a hydrophobic crevice made up of the side chains of Ile 104 and 107, the aliphatic portions of Asn 204 and 206, and the hexyl moiety of the bound inhibitor. There is a hydrogen bonding interaction between the hydroxyl group of Tyr 108 and the amide nitrogen of Gly 205. The α-carbon atoms of the wild-type (A. J. Oakley *et al*., unpublished results) and Y108F mutant models superimpose using the algorithm of Rossmann and Argos (1975) with a rms deviation of 0.16 Å. There is no significant movement of either main chain or side chain atomic positions within a 10 Å sphere of the mutation (Figure 2), and no significant movement of the aromatic ring of Phe 108. Despite these crystallographic observations, the substitution of Tyr 108 with Phe greatly affects the catalytic properties of GST P1-1 toward a number of substrates, as discussed below.

Effect of the Removal of the Hydroxyl Group of Tyr 108 on Catalysis with Ethacrynic Acid as a Substrate. Among GST isoenzymes, GST P1-1 displays the highest activity with EA. Kinetic data and viscosity experiments presented here clearly indicate that, like with CDNB (Ricci *et al*., 1996) and NBD-Cl (Caccuri *et al*., 1996), the GST P1-1-catalyzed reaction between EA and GSH follows a rapid equilibrium random sequential bi−bi kinetic mechanism with a rate-limiting step localized after the binding of the two substrates and before the release of products. In a manner similar to that observed with CDNB (Ivanetich & Goold, 1989), a negative intrasubunit synergistic modulation of one substrate on the binding of the second one occurs (coupling factor α = 1.6). Replacement of Tyr 108 with Phe sheds light on the function of this residue in this enzymatic conjugation. Tyr 108 is in a structurally conserved position within the mu, pi, and theta classes and appears to be one of the few polar residues contributing to the H site. It has also been suggested previously that Tyr 115 (the equivalent residue in the mu class) may assist, through its hydroxyl group, in stabilizing the enol or enolate intermediate in Michael addition reactions (Ji *et al*., 1994). Kinetic data for GST P1-1 are all consistent with this hypothesis as k_{cat} is lowered about 14-fold in Y108F and no changes in the kinetically important acid−base equilibria have been observed in the ternary complex (data not shown). Crystallographic analysis of GST P1-1 in complex with EA (Oakley *et al.*, 1997) shows that this substrate is bound to the H site in a nonproductive manner in the binary complex. On the contrary, the three-dimensional structure of GST P1-1 in complex with GS-EA indicates a completely different orientation of EA with its carbonyl oxygen in incipient hydrogen bonding geometry of Tyr 108 (the two groups are 3.0 Å distant but they lie parallel to one another) or in a water-mediated hydrogen bond which displays a better geometry. These structural data, combined with kinetic data, fulfill a possible scenario of catalysis; binding of GSH may produce an induced fit transition which also involves the H site and which locates EA in a productive manner. This is not surprising as an induced fit mechanism by GSH has been recently observed for GST P1-1 (Ricci *et al*., 1996). Now, the hydroxyl function of Tyr 108 may assist the Michael addition by stabilizing the enolate of EA through a hydrogen bonding interaction with the carbonyl group of EA. The observation that the substitution of Tyr 108 with Phe does not alter the affinity of the H site for EA indicates that an incipient hydrogen bond between Tyr 108 and EA is more likely than a stronger water-mediated hydrogen bond. This incipient hydrogen bond could become stronger during the transition state. Moreover, the observed decrease of the k_{cat}/K_m^{GSH} and k_{cat}/K_m^{EA} ratios in the mutant ruled out the possibility that Tyr 108 may act to locate EA (or GSH) in a correct orientation in the active site; otherwise, in the case of nonproductive substrate binding produced by this point mutation, we would expect unchanged k_{cat}/K_m values (Fersht, 1985).

Similar general conclusions about the effect of this residue on EA conjugation have been reported by Barycki and Colman (1993) using an affinity labeling approach for the class mu enzyme (isozyme 4-4). Tyr 115 (the counterpart of Tyr 108 in class pi) was reacted with 4-(fluorosulfonyl)-benzoic acid. This chemical modification yielded a 4-fold decrease of k_{cat} in the EA/GSH system and a modest change of the apparent K_m^{EA} value. These kinetic data have been interpreted as a direct involvement of Tyr 115 in catalysis rather than facilitating the binding of the xenobiotic substrate. Very recently, Ji *et al*. (1995) mutated the sigma class squid GST residue F106 to Tyr (the residue equivalent to Y108 in GST P1-1 and Y115 in the μ class) and found an increased efficiency of the enzyme in the Michael addition of GSH to 4-phenyl-3-buten-2-one. It is worth noting that, in the alpha class GST (where the residue equivalent to Tyr 108 is Val 111), the specific activity with ethacrynic acid is very low, consistent with the importance of the tyrosine residue for Michael addition reactions. The fact that there is still some activity in the alpha class enzyme, even though it is much lower compared to that of other GST classes, was recently discussed by Cameron *et al*. (1995), who suggested that the role of the general acid in the Michael addition with this enzyme could be played by a nearby residue such as Tyr 9, Arg 15 (N_ϵ atom), or a water molecule located close to the substrate. The residual activity toward EA of the Tyr 108 to Phe mutant may be due to a water molecule we observe in the wild-type complex with GS-EA (Oakley *et al*., 1997), in which the water molecule is positioned within hydrogen bonding distance of both Y108 and the carbonyl of EA. The same water molecule is observed in other complexes of the enzyme, including the Y108F crystal structure, where it is hydrogen bonded to other water molecules in the H site.

Effect of the Removal of the Hydroxyl Group of Tyr 108 on Catalysis with NBD-Cl. The effect of mutation of Tyr 108 into Phe, using NBD-Cl as the substrate, appears to be very different from that seen in the EA/GSH system. The Y108F mutant enzyme shows a significant increase in K_m values toward NBD-Cl and GSH and a k_{cat} value 7-fold higher than that of wild-type enzyme (Table 4). These findings suggest a negative influence of the hydroxyl group

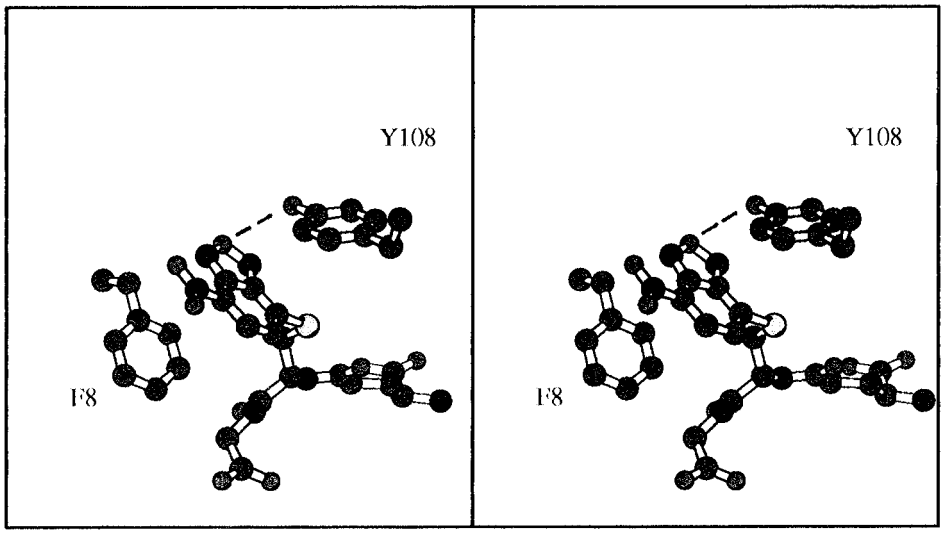

FIGURE 7: Stereofigure of the glutathione conjugate of NBD-Cl bound in the H site of human class π GST P1-1. The figure was derived from coordinates based on modeling the substrate into the crystal structure of the enzyme as described in Experimental Procedures. The figure was generated with the program MOLSCRIPT (Kraulis, 1991).

on this catalysis and a positive contribution on the affinity of the enzyme for both GSH and NBD-Cl.

Recent studies on the catalytic mechanism of GST P1-1, either with NBD-Cl or with CDNB as cosubstrates, may help to explain this different effect caused by Tyr 108. It has been suggested that the rate-limiting step with both compounds is a physical event probably involving structural transitions of the ternary complex (Ricci *et al*., 1996; Caccuri *et al*., 1996). In the case of CDNB, diffusion-controlled motions of helix 2 and helix 4 are possibly involved in the k_{cat} and in the K_m^{GSH} modulation (Ricci *et al*., 1996). In the case of NBD-Cl, k_{cat} seems related to slow and then non-diffusion-controlled motions of helix 4; the observed low k_{cat} value and its viscosity independence have been interpreted as being caused by an increased rigidity of helix 4 (Caccuri *et al*., 1996). Now, molecular modeling shows the heterocyclic portion of NBD-Cl packed against the aromatic rings of Tyr 108 and Phe 8 and the hydroxyl group of Tyr 108 within hydrogen bonding distance of the oxygen atom of NBD-Cl (Figure 7). Just this additional link could produce an increased internal friction and then could be responsible for the low and viscosity-independent k_{cat} value, and of the high affinity for NBD-Cl as well. In addition, the structural constraint caused by this additional bond seems to be transmitted to the G site, via helix 4, yielding an increased affinity for GSH ($K_m^{GSH} = 8\ \mu M$). All kinetic data reported here for Y108F support these suggestions. Removal of the hydroxyl function of Tyr 108 causes a 7-fold increase in the k_{cat} value (Table 4) and a concomitant decrease of the affinity both for NBD-Cl and for GSH ($K_m^{GSH} = 55\ \mu M$ and $K_m^{NBD-Cl} = 32\ \mu M$ in Y108F; $K_m^{GSH} = 8\ \mu M$ and $K_m^{NBD-Cl} = 4\ \mu M$ in WT). These results are all consistent with the involvement of Tyr 108 in the binding of NBD-Cl, in the synergic modulation of G and H sites, and in an unfavorable modulation of k_{cat}, probably due to less flexibility of helix 4. The possibility that the incresed k_{cat} for Y108F is due to a changed pH depencence of kinetically important ionizations may be ruled out (see Figure 5). However, it is evident that the hydrogen bond between Tyr 108 and NBD-Cl is just one of the factors modulating the helix 4 flexibility as a further 8-fold increase in k_{cat} is required to reach a k_{cat} value similar to that observed with CDNB. In addition, the affinity of Y108F for GSH and NBD-Cl is still 3- and 30-fold higher than that observed for GSH and CDNB. Thus, other interactions of the H site with NBD-Cl, and not present with CDNB, are likely.

Because the k_{cat}/K_m^{NBD-Cl} ratio does not differ appreciably between the mutant and WT enzymes, a completely different explanation of the above data may be given by assuming that removal of the hydroxyl function of Tyr 108 yields a more productive binding of NBD-Cl. Comparison of the viscosity effect on the kinetics of Y108F and of wild-type enzyme in the presence of CDNB or NBD-Cl provides critical information in this context. With CDNB as the cosubstrate, k_{cat} is viscosity-dependent in WT, and this dependence is very similar to that found with Y108F (Figure 6 and Table 3); this confirms that the hydroxyl function of Tyr 108 does not interact with CDNB and does not alter the diffusion-dependent motions of protein regions (probably helix 4) which are related to the rate-limiting step in catalysis. On the contrary, with NBD-Cl as the cosubstrate, the mutated enzyme shows a viscosity dependence of k_{cat} which is nearly absent in the wild-type enzyme (Figure 6 and Table 3). This provides a strong indication that the enzyme, after removal of the hydroxyl group of Tyr 108, becomes more flexible and functionally important motions are now diffusion-controlled and viscosity-dependent. The appearance of a viscosity dependence of k_{cat} in Y108F would be difficult to explain if this point mutation only caused a more productive binding of NBD-Cl. The fact that the k_{cat} modulation by viscosity of Y108F with NBD-Cl is not as high ($\alpha = 0.38$) as that observed with CDNB ($\alpha = 0.81$) indicates again that other additional interactions with NBD-Cl could be present in the mutant which partially limit the flexibility of helix 4.

All these suggestions about the negative role of Tyr 108 in the GSH/NBD-Cl system are indirectly supported by the kinetic properties that the mu and alpha GSTs exhibit toward NBD-Cl. In fact, the mu GST, which has Tyr 115 as the equivalent residue of the pi class, displays very low k_{cat} values like the pi isoenzyme; on the contrary, the α GST, in which a Val residue replaces Tyr 108, shows a very high catalytic efficiency similar to that found with CDNB (Ricci *et al*., 1994).

Effect of the Removal of the Hydroxyl Group of Tyr 108 on Catalysis with CDNB, DTNB, and 4NQO as Substrates. There is little effect of this point mutation on the reaction with CDNB, DTNB, and 4NQO as there is a small decrease in the k_{cat} values, while the K_m values remain unchanged (Table 4). These results suggest that, in these nucleophilic aromatic substitutions and thiol disulfide exchange reactions, the hydroxyl group of Tyr 108 is involved neither in the rate-limiting step nor in the binding of these cosubstrates. Modeling of GST P1-1 in complex with the GSH conjugate with CDNB shows the cosubstrate packed between Phe 8 and Tyr 108 aromatic rings, but no specific interaction between the hydroxylic portion of Tyr 108 can be seen (A. J. Oakley *et al*., unpublished results). Similarly, Pennington and Rule (1992) mutated Tyr 116 of human muscle class mu GST to Phe and did not observe any decrease in the specific activity of the enzyme toward CDNB. These last results are again consistent with the idea that the contribution of this residue in the CDNB/GSH system is solely to provide hydrophobic interactions through the aromatic ring of the tyrosine residue. The results reported by Barycki and Colman (1993) concerning chemical modification of rat GST, isozyme 4-4 (class mu) with 4-(fluorosulfonyl)benzoic acid (4-FSB), indicated that the K_m for CDNB increased 9-fold and the k_{cat} decreased over 4-fold. These authors interpreted these results by suggesting that Tyr 115 may position the C(1) atom of CDNB in proximity to the thiolate anion of GSH only by providing hydrophobic interactions through the benzene ring of the substrate. A different result has been reported by Johnson *et al*. (1993), who studied the role of the equivalent residue in isozyme 3-3 of rat GST (class mu) using CDNB as a second substrate. They found in the Y115F mutant enzyme an increase in the k_{cat} value of about 3-fold compared to that of the wild-type enzyme. This higher catalytic efficiency was explained with the removal of the hydroxyl function of Tyr 115 which, in hydrogen bonds by the main chain NH moiety of Ser 209, limits the product release (rate-limiting). All these experimental results demonstrate that Tyr 108, and its equivalent in the other GST classes, can play different roles within and between GST isoenzyme families.

REFERENCES

Armstrong, R. N. (1994) in *Advances in Enzymology and Related Areas of Molecular Biology* (Meister, A., Ed.) pp 1−44, John Wiley & Sons, New York.

Awasthi, S., Srivastava, S. K., Ahmad, F., Ahmad, H., & Ansari, G. A. S. (1993) *Biochim. Biophys. Acta 1164*, 173−178.

Bammler, T., Driessen, H., Finnstrom, N., & Wolf, C. R. (1995) *Biochemistry 34*, 9000−9008.

Barycki, J. J., & Colman, R. F. (1993) *Biochemistry 32*, 13002−13011.

Batist, G., Tulpule, A., Sinha, B. K., Katki, A. G., Myers, C. E., & Cowan, K. H. (1986) *J. Biol. Chem. 261*, 15544−15549.

Battistoni, A., Mazzetti, P., Petruzzelli, R., Muramatsu, M., Ricci, G., Federici, G., & Lo Bello, M. (1995) *Protein Expression Purif. 6*, 579−587.

Black, S. M., Beggs, J. D., Hayes, J. D., Bartoszek, A., Muramatsu, M., Sakai, M., & Wolf, C. R. (1990) *Biochem. J. 268*, 309−315.

Brünger, A. T., Kuriyan, J., & Karplus, M. (1987) *Science 235*, 458−460.

Buetler, T. M., & Eaton, D. L. (1992) *Environ. Carcinog. Ecotoxicol. Rev. 10*, 181−203.

Caccuri, A. M., Ascenzi, P., Lo Bello, M., Federici, G., Battistoni, A., Mazzetti, P., & Ricci, G. (1994) *Biochem. Biophys. Res. Commun. 200*, 1428−1434.

Caccuri, A. M., Ascenzi, P., Antonini, G., Parker, M. W., Oakley, A. J., Chiessi, E., Nuccetelli, M., Battistoni, A., Bellizia, A., & Ricci, G. (1996) *J. Biol. Chem. 271*, 16193−16198.

Cameron, A. D., Sinning, I., L'Hermite, G., Olin, B., Board, P. G., Mannervik, B., & Jones, T. A. (1995) *Structure 3*, 717−727.

CCP4 Suite (1994) *Acta Crystallogr. D 50*, 750−763.

Ellman, G. L. (1959) *Arch. Biochem. Biophys. 82*, 70−77.

Fersht, A. (1985) *Enzyme Structure and Mechanism*, 2nd ed., pp 109−111, W. H. Freeman and Co., New York.

Garcìa-Saez, I., Pàrraga, A., Phillips, M. F., Mantle, T. J., & Coll, M. (1994) *J. Mol. Biol. 237*, 298−314.

Habig, W. H., Pabst, M. T., & Jakoby, W. B. (1974) *J. Biol. Chem. 249*, 7130−7139.

Ivanetich, K. M., & Goold, R. D. (1989) *Biochim. Biophys. Acta 998*, 7−13.

Jakoby, W. B., & Habig, W. H. (1980) in *Enzymatic Basis of Detoxification* (Jakoby, W. B., Ed.) Vol. 2, pp 63−94, Academic Press, New York.

Ji, X., Zhang, P., Armstrong, R. N., & Gilliland, G. L. (1992) *Biochemistry 31*, 10169−10184.

Ji, X., Johnson, W. W., Sesay, M. A., Dickert, L., Prasad, S. M., Ammon, H. L., Armstrong, R. N., & Gilliland, G. L. (1994) *Biochemistry 33*, 1043−1052.

Ji, X., von Rosenvinge, E. C., Johnson, W. W., Tomarev, S. I., Piatigorsky, J., Armstrong, R. N., & Gilliland, G. L. (1995) *Biochemistry 34*, 5317−5328.

Johnson, W. W., Liu, S., Ji, X., Gilliland, G. L., & Armstrong, R. N. (1993) *J. Biol. Chem. 268*, 11508−11511.

Kano, T., Sakai, M., & Muramatsu, M. (1987) *Cancer Res. 47*, 5626−5630.

Kleywegt, G., & Jones, T. A. (1994) in *From First Map to Final Model* (Bailey, S., Hubbard, R., & Waller, D., Eds.) pp 59−66, EPSRC Daresbury Laboratory, Warrington, U.K.

Kong, K. H., Inoue, H., & Takahashi, K. (1992) *J. Biochem. 112*, 725−728.

Kramer, B., Kramer, W., & Fritz, M. J. (1984) *Cell 38*, 879−887.

Kraulis, J. P. (1991) *J. Appl. Crystallogr. 24*, 946−950.

Kunkel, T. A., Bebenek, K., & McClary, J. (1991) *Methods Enzymol. 204*, 125−139.

Laemmli, U. K. (1970) *Nature 227*, 680−685.

Laskowski, R. A., McArthur, M. W., Moss, D. S., & Thorton, J. M. (1993) *J. Appl. Crystallogr. 26*, 282−291.

Liu, S., Zhang, P., Ji, X., Johnson, W. W., Gilliland, G. L., & Armstrong, R. N. (1992) *J. Biol. Chem. 267*, 4296−4299.

Lo Bello, M., Battistoni, A., Mazzetti, A. P., Board, P. G., Muramatsu, M., Federici, G., & Ricci, G. (1995) *J. Biol. Chem. 270*, 1249−1253.

Lowry, O. H., Rosebrough, N. J., Farr, A. L., & Randall, R. J. (1951) *J. Biol. Chem. 193*, 265−275.

Mannervik, B., Ålin, P., Guthenberg, C., Jensson, H., Tahir, M. K., Warholm, M., & Jörnvall, H. (1985) *Proc. Natl. Acad. Sci. U.S.A. 82*, 7202−7206.

Mannervik, B., Awasthi, Y. C., Board, P. G., Hayes, J. D., Di Ilio, C., Ketterer, B., Listowsky, I., Morgerstern, R., Muramatsu, M., Pearson, W. R., Pickett, C. B., Sato, K., Widersten, M., & Wolf, C. D. (1992) *Biochem. J. 282*, 305−308.

Manoharan, T. H., Gulick, A. M., Reinemer, P., Dirr, H. D., Huber, R., & Fahl, W. H. (1992) *J. Mol. Biol. 226*, 319−322.

McPherson, A. (1982) *The Preparation and Analysis of Protein Crystals*, Wiley, New York.

Meyer, D. J., Coles, B., Pemble, S. E., Gilmore, K. S., Fraser, G. M., & Ketterer, B. (1991) *Biochem. J. 274*, 409−414.

Oakley, A. J., Rossjohn, J., Lo Bello, M., Caccuri, A. M., Federici, G., & Parker, M. W. (1997) *Biochemistry 36*, 576−585.

Otwinowski, Z. (1993) in *Data Collection and Processing* (Sawyer, L., Isaacs, N., & Bailey, S., Eds.) pp 56−62, SERC Daresbury Laboratory, Warrington, U.K.

Parker, M. W., Lo Bello, M., & Federici, G. (1990) *J. Mol. Biol. 213*, 221−222.

Pennington, C. J., & Rule, G. S. (1992) *Biochemistry 31*, 2912−2920.
Phillips, M. F., & Mantle, T. J. (1991) *Biochem. J. 275*, 703−709.
Ploemen, J. H. T. M., van Hommen, B., & van Bladeren, P. J. (1990) *Biochem. Pharmacol. 40*, 1631−1635.
Puchalski, R., & Fahl, W. E. (1990) *Proc. Natl. Acad. Sci. U.S.A. 87*, 2443−2447.
Read, R. J. (1986) *Acta Crystallogr. A 42*, 140−149.
Reinemer, P., Dirr, H. W., Ladenstein, R., Schaffer, J., Gallay, O., & Huber, R. (1991) *EMBO J. 10*, 1997−2005.
Reinemer, P., Dirr, H. W., Ladenstein, R., Huber, R., Lo Bello, M., Federici, G., & Parker, M. W. (1992) *J. Mol. Biol. 227*, 214−226.
Ricci, G., Caccuri, A. M., Lo Bello, M., Pastore, A., Piemonte, F., & Federici, G. (1994) *Anal. Biochem. 218*, 463−465.
Ricci, G., Caccuri, A. M., Lo Bello, M., Rosato, N., Mei, G., Nicotra, M., Chiessi, E., Mazzetti, A. P., & Federici, G. (1996) *J. Biol. Chem. 271*, 16187−16192.
Rossmann, M. G., & Argos, P. (1975) *J. Biol. Chem. 250*, 7525−7532.
Segel, I. H. (1975) *Enzyme Kinetics*, John Wiley & Sons, New York.
Simmons, P. C., & Van der Jagt, D. L. (1977) *Anal. Biochem. 82*, 334−341.
Sinning, I., Kleywegt, G. J., Cowan, S. W., Reinemer, P., Dirr, H. W., Huber, R., Gilliland, G. L., Armstrong, R. N., Ji, X., Board, P. G., Olin, B., Mannervik, B., & Jones, T. A. (1993) *J. Mol. Biol. 232*, 192−212.
Stanley, J. S., & Benson, A. M. (1988) *Biochem. J. 256*, 303−306.
Tsuchida, S., Sekine, Y., Shineha, R., Nishihira, T., & Sato, K. (1989) *Cancer Res. 49*, 5225−5229.
Widersten, M., Kolm, R. H., Bjornstedt, R., & Mannervik, B. (1992) *Biochem. J. 285*, 377−381.
Widersten, M., Björnestedt, R., & Mannervik, B. (1994) *Biochemistry 33*, 11717−11723.
Wilce, M. C. J., Board, P. G., Feil, S. C., & Parker, M. W. (1995) *EMBO J. 14*, 2133−2143.
Wolf, A. V., Brown, M. G., & Prentiss, P. G. (1985) in *Handbook of Chemistry and Physics* (Weast, R. C., Astle, M. J., & Beyer, W. H., Eds.) pp D219−D269, CRC Press, Inc., Boca Raton, FL.
Yang, W. Z., Begleiter, A., Johnston, J. B., Israels, L. G., & Mowat, M. R. (1992) *Mol. Pharmacol. 41*, 625−630.
Zimniak, P., Nanduri, B., Pikula, S., Bandorowicz-Pikula, J., Singhal, S. S., Srivastava, S. K., Awasthi, S., & Awasthi, Y. C. (1994) *Eur. J. Biochem. 224*, 893−899.

BI962813Z